Porous Materials

DOI: 10.1002/anie.201107906

Inverse and High CO_2/C_2H_2 Sorption Selectivity in Flexible Organic–Inorganic Ionic Crystals**

*Ryo Eguchi, Sayaka Uchida, and Noritaka Mizuno**

Carbon dioxide storage and separation is a topical research area in terms of environmental protection and industrial processes.[1] In particular, the removal of CO_2 from industrial gases is an essential process because CO_2 is commonly present as an impurity in many industrial processes. Acetylene (C_2H_2) is one of the most important gases and is used as a key starting material for various fine chemicals and electronic materials.[2] C_2H_2 is mainly produced by thermal cracking of hydrocarbons, which produces a large amount of byproducts, including CO_2.[2a] Therefore, the purification of C_2H_2 by the removal of CO_2 is technologically of great importance. The separation of CO_2 by porous materials has received much attention as a promising method owing to its energetic benefit.[1,3] However, owing to very similar sizes, shapes, and physical properties of CO_2 (kinetic diameter 3.3 Å, b.p. 194.7 K) and C_2H_2 (3.3 Å, 189.2 K; Supporting Information, Table S1), conventional porous materials such as zeolites and carbon materials can hardly distinguish these two molecules (Supporting Information, Table S2).[4]

Recently, a new class of porous materials, composed of transition-metal ions and organic ligands such as metal–organic frameworks (MOFs) and porous coordination polymers (PCPs), has been intensively investigated for the storage and separation of gases.[5] Their structural designability and flexibility lead to the unique characters and are the origin of their unprecedented gas sorption properties.[6] Several MOFs/PCPs demonstrate high C_2H_2 sorption selectivity over CO_2 by precise control and functionalization of the pore walls: oxygen atoms and unsaturated metal ions can work as hydrogen-bonding and Lewis acid sites, respectively.[7–9] On the other hand, there are few examples of MOFs/PCPs with high CO_2 sorption selectivity over C_2H_2 that take advantage of the structural flexibility.[10]

Ionic crystals are constructed with anions and cations, which create strong electrostatic fields at the internal surfaces that are suitable for accommodating polar molecules.[10a,11] The Coulomb potential generated by the ionic components is isotropic and decreases with the inverse distances. Thus, some ionic crystals can transform their crystal structures to be adapted to specific guest molecules.[11c,d] CO_2 and C_2H_2 are nonpolar molecules, and the respective polar C=O and C–H bonds are oriented in opposite directions. Calculation of ESP charges[12] showed that CO_2 (C + 0.700 e, O −0.350 e) was more polarized than C_2H_2 (C −0.266 e, H + 0.266 e; Supporting Information, Table S3). Therefore, the strong electrostatic fields and structural flexibility of ionic crystals are potentially suitable for accommodating CO_2 and distinguishing CO_2 from C_2H_2. Polyoxometalates (POMs) are anionic nanosized metal–oxygen clusters that form nanostructured ionic crystals with unique guest sorption properties by complexation with appropriate organometallic cations (macrocations).[11a–c,13] Based on these ideas, a flexible organic–inorganic ionic crystal $K_2[Cr_3O(OOCH)_6(4\text{-ethylpyridine})_3]_2[\alpha\text{-}SiW_{12}O_{40}]\cdot 4\,CH_3OH$ (**1**·4 CH_3OH) was synthesized by complexation of silicododecatungstates $[\alpha\text{-}SiW_{12}O_{40}]^{4-}$, macrocations $[Cr_3O(OOCH)_6(4\text{-ethylpyridine})_3]^{+}$, and potassium ions. Compound **1** showed high affinity toward CO_2, and the CO_2 sorption proceeded by two phase transitions, while the C_2H_2 sorption proceeded by a single phase transition. The CO_2/C_2H_2 sorption amount ratio reached up to the highest value of 4.8 (278 K, 100 kPa).

The crystal structure of **1**·4 CH_3OH (*ab* plane) is shown in Figure 1a. Silicododecatungstates and macrocations were lined up along the *c* axis, forming struts. The distance between pyridine rings of the neighboring macrocations was 4.04(2) Å,

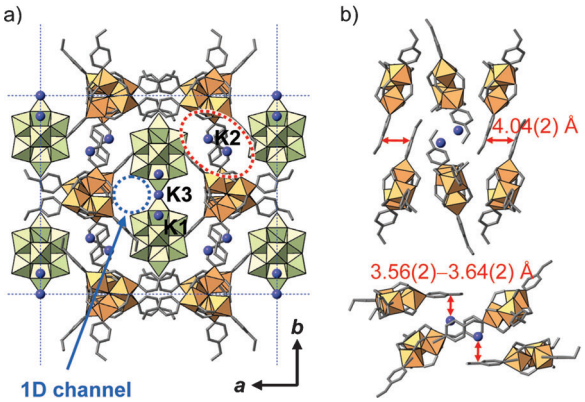

Figure 1. Crystal structure of **1**·4 CH_3OH. a) Arrangements of the constituent ions in the *ab* plane and b) local structure of the space surrounded by the etpy ligands, showing π–π (top) and cation–π interactions (bottom). Green and orange polyhedra represent the WO_6 and CrO_5N units, respectively; purple spheres: potassium ions; blue dashed circle and red dashed oval: the channel and space surrounded by the etpy ligands, respectively. C–C, C–O, and C–N bonds: gray. Solvent methanol molecules omitted for clarity.

[*] R. Eguchi, Dr. S. Uchida, Prof. Dr. N. Mizuno
Department of Applied Chemistry, School of Engineering
The University of Tokyo, 7-3-1 Hongo, Bunkyo-ku, Tokyo (Japan)
E-mail: tmizuno@mail.ecc.u-tokyo.ac.jp

[**] This work was supported by the Global COE Program (Chemistry Innovation through Cooperation of Science and Engineering), the Development in a New Interdisciplinary Field Based on Nanotechnology and Materials Science Programs, and Grants-in-Aid for Scientific Research from the Ministry of Education, Culture, Science, Sports, and Technology of Japan.

Supporting information for this article is available on the WWW under http://dx.doi.org/10.1002/anie.201107906.

with π–π interactions (Figure 1b, top). The struts were assembled in the *ab* plane to form one-dimensional channels along the *c* axis. The diameter of the channel aperture was 3.5 Å. Calculation with the PLATON program[14] showed that there were two kinds of accessible spaces. One was a one-dimensional channel (shown by the blue dashed circle in Figure 1a), and the volume was about 250 Å^3 per formula unit. The other was a space surrounded by four 4-ethylpyridine (etpy) ligands (red dashed oval in Figure 1a), which was accessible from the one-dimensional channel, and the volume was about 100 Å^3 per formula unit. Therefore, the total void volume of **1**·4 CH_3OH was about 350 Å^3 per formula unit (13% of the crystal volume). Two potassium ions per formula unit were disordered among three positions K1, K2, and K3 with occupancies of 0.6, 0.5, and 0.4, respectively, and were located either in the vicinity of silicododecatungstates (K1 and K3) or in the space surrounded by the etpy ligands (K2). One potassium ion per formula unit (K2) existed in the space surrounded by the etpy ligands and interacted with two etpy ligands (K2–C 3.56(2)–3.64(2) Å), with weak cation–π interactions (Figure 1b, bottom). The solvent methanol molecules existed in the one-dimensional channels and were in the vicinity of potassium ions (K1 or K3–O ca. 2.8 Å).

Thermogravimetric (TG) analysis of **1**·4 CH_3OH showed complete desorption of the guest methanol molecules at 373 K (Supporting Information, Figure S1). Therefore, the guest-free phase **1** was obtained by the treatment of **1**·4 CH_3OH at 373 K in vacuo. Rietveld refinement[15–17] of **1** (Supporting Information, Figure S2; $R_p = 1.21$, $R_{wp} = 1.78$) showed a slightly different framework structure from that of **1**·4 CH_3OH, and a decrease in the unit cell volume (ca. −6.0%; Figure 2 and Table 1). The channel diameter was largely decreased from 3.5 Å (**1**·4 CH_3OH) to 2.6 Å (**1**; Supporting Information, Figure S3). The XRD pattern of **1**·4 CH_3OH was restored by the exposure of **1** to the methanol vapor, showing the reversible phase transition (Supporting Information, Figure S4).

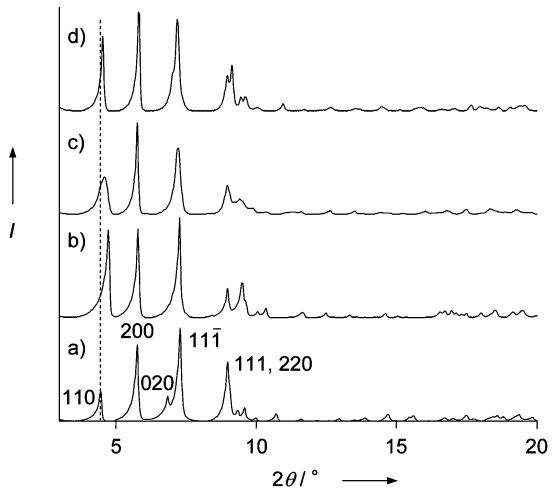

Figure 2. Powder XRD patterns of a) **1**·4 CH_3OH, b) **1**, c) **1**·0.6 CO_2, and d) **1**·3 CO_2. The Miller indices of the main diffraction peaks are shown for (a).

Table 1: Lattice parameters and unit cell volumes of **1**·3 CO_2, **1**·0.6 CO_2, **1**, and **1**·4 CH_3OH.[a]

	a [Å]	*b* [Å]	*c* [Å]	*V* [Å^3]
1·3 CO_2	32.166(6)	24.989(5)	13.960(2)	10482
1·0.6 CO_2	32.75(1)	24.109(9)	14.164(5)	10378
1	32.544(4)	23.419(3)	14.200(1)	10104
1·4 CH_3OH	32.2376(2)	25.4443(2)	13.9464(2)	10747

[a] The space group of these phases was *C*2/*c*.

The sorption property of **1** was investigated by sorption–desorption isotherms (Figure 3). Compound **1** exhibited surface sorption only for N_2, O_2, and CO at 77 K, probably because the aperture of **1** (2.6 Å) was smaller than their molecular sizes (3.46–3.76 Å; Supporting Information,

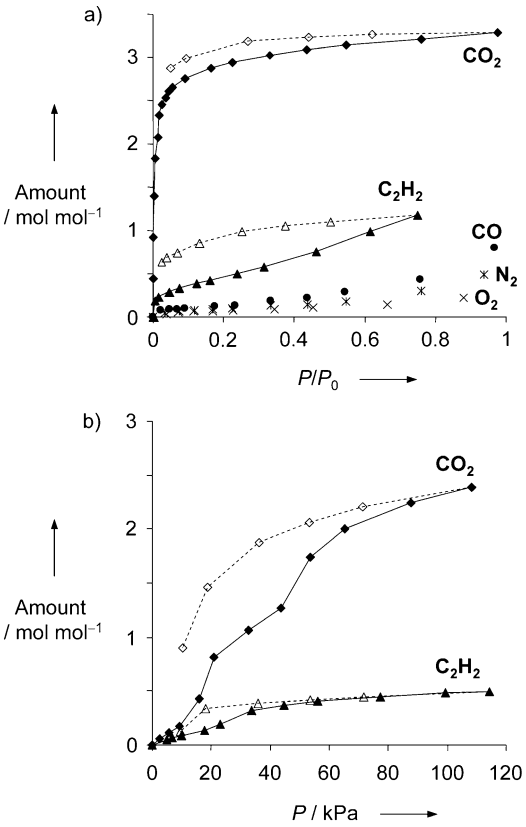

Figure 3. Gas sorption isotherms of **1** at a) 77 K (CO, N_2, and O_2) and 195 K (CO_2 and C_2H_2), and b) 278 K. Closed and open symbols indicate the sorption and desorption branches, respectively. Saturation pressures (P_0) of N_2, O_2, CO, CO_2, and C_2H_2 are 101.3, 20.7, 60.0, 101.3, and 143.8 kPa, respectively.

Table S1). However, CO_2 and C_2H_2 sorption isotherms at 195 K were type I (IUPAC classification) indicative of physisorption by microporous materials, despite their molecular sizes being larger than the aperture of **1**. The saturated amounts of CO_2 and C_2H_2 sorption were 3 and 1 mol mol^{-1}, respectively, and **1** in particular showed high affinity toward CO_2. Essentially the same isotherms as those of the first run were obtained after four cycles. The BET surface area calculated from the CO_2 sorption isotherm was 75 m^2 g^{-1}.

The sorption isotherm of CO_2 at 278 K consisted of two steps and a large hysteresis loop, suggesting a guest-induced phase transition.[6,18,19] The sorption isotherm of C_2H_2 consisted of a single step and a hysteresis loop, while the amount of sorption was smaller. The CO_2/C_2H_2 sorption amount ratio reached up to 4.8 at 278 K and 100 kPa and is the inverse and highest selectivity relative to those of zeolites, carbon materials, and MOFs/PCPs (0.3–1.9 under moderate conditions;[4,7–10] Supporting Information, Table S2).

To investigate the nature of the high CO_2/C_2H_2 sorption selectivity, N_2O was chosen as a reference molecule, as the structural and physical properties (kinetic diameter 3.3 Å, b.p. 184.7 K) are similar to those of CO_2 and C_2H_2 (Supporting Information, Table S1). The N_2O sorption isotherm at 278 K also possessed a single step and a hysteresis loop. The amounts of sorption decreased in the order $CO_2 > N_2O > C_2H_2$ (Supporting Information, Figure S5). Calculation of the ESP charges[12] showed that the polarization extent decreased in the same order of $CO_2 > N_2O > C_2H_2$ (Supporting Information, Table S3). Therefore, the polarity of guest molecules would play a crucial role in the sorption behavior of **1**.

To obtain further information on the sorption mechanism, sorption enthalpies of CO_2 and C_2H_2 were calculated and plotted with the Clausius–Clapeyron equation[20] (Figure 4).

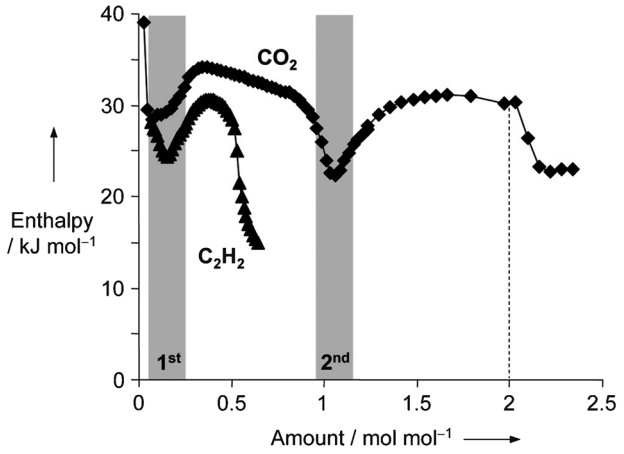

Figure 4. Sorption enthalpy plots of CO_2 and C_2H_2 against the amounts of sorption. Two valleys are highlighted in gray.

The plot of CO_2 showed significant valleys at the amounts of 0.1 and 1 mol mol^{-1} that are obviously different from typical plots of rigid microporous materials. Valleys have been reported to be indicative of additional heat required for a phase transition of host materials.[19] The energies for first and second phase transition were estimated to be about 4 and 9 kJ mol^{-1}, respectively. The enthalpies of the two plateaus were relatively high and close to each other (30–35 kJ mol^{-1}). Notably, the sorbed amounts at the end of the first and second plateaus were one and two CO_2 molecules per formula unit, respectively. Compound **1** possessed two potassium ions per formula unit that resided in distinct places (spaces surrounded by the etpy ligands and one-dimensional channels along the *c* axis). The CO_2 sorption enthalpies for alkali metal ion-exchanged zeolites (for example, Zeolite 13X and SAPO-34) are reported to be about 30–40 kJ mol^{-1}.[22] Therefore, the phase transition is probably induced by the CO_2 binding to the two potassium ions per formula unit that reside in distinct places. On the other hand, the sorption enthalpy plot of C_2H_2 showed one valley (0.2 mol mol^{-1}) that is indicative of a single phase transition, and the sorption enthalpy of C_2H_2 was smaller than that of CO_2. These results suggest that the strong interaction between CO_2 and potassium ions induces the two-step phase transition, resulting in the highly selective sorption of CO_2 over C_2H_2.

The two-step phase transition accompanying the sorption of CO_2 was directly observed by in situ XRD measurements under a CO_2 atmosphere (Figure 2). The XRD patterns of **1**·0.6 CO_2 (299 K, 50 kPa) and **1**·3 CO_2 (233 K, 80 kPa), which correspond to the phases after the first and second phase transitions, respectively, were different from each other and that of **1**.[23,24] These lattice parameters were determined by the Pawley refinements[15,16] (Table 1; Supporting Information, Figure S7). The unit cell volume increased by the sorption of CO_2: 10104 Å^3 (**1**)→10378 Å^3 (**1**·0.6 CO_2)→10482 Å^3 (**1**·3 CO_2). The increase in the lattice volume of **1** by the sorption of 3 mol mol^{-1} of CO_2 was 378 Å^3, and the value was comparable to the volume of 3 mol mol^{-1} of CO_2 (403 Å^3). The XRD pattern also changed from **1** to **1**·0.4 C_2H_2 (298 K, 90 kPa), and the unit cell volume increased to 10391 Å^3 (Supporting Information, Figure S8). However, a further change of the XRD pattern was not observed by cooling the sample to about 233 K. These results suggest that **1** accommodates CO_2 molecules by expanding its lattice by two steps and shows higher structural flexibility for the sorption of CO_2 than that of C_2H_2.

Monte Carlo simulation combined with periodic DFT calculation was carried out to elucidate the CO_2 binding sites in more detail. The calculated geometry of CO_2 (1 mol mol^{-1}) sorbed in **1** is shown in the Supporting Information, Figure S9. CO_2 molecules resided in the space surrounded by the etpy ligands and interacted with potassium ions (K–O = 2.638, 2.644 Å). Therefore, sorbed CO_2 molecules would initially interact with the potassium ions in the space surrounded by the etpy ligands and subsequently with the potassium ions in the one-dimensional channels.[25]

In summary, we have synthesized a flexible organic–inorganic ionic crystal **1** that demonstrates inverse and high CO_2/C_2H_2 sorption selectivity. The key for the high affinity toward CO_2 is the combination of structural flexibility and strong binding sites (that is, potassium ions). The structural flexibility and strong electrostatic field of the ionic crystals will pave the way for unique sorption properties.

Experimental Section

Syntheses of **1**·4 CH_3OH and **1**: $[Cr_3O(OOCH)_6(4\text{-ethylpyridine})_3](ClO_4)\cdot n\,H_2O$[26] (0.50 g) was dissolved in 1,2-dichloroethane (100 mL), and then CH_3COOK (0.50 g) dissolved in a minimum amount of methanol (ca. 2 mL) was added. This solution was filtered to remove $KClO_4$ (solution A). $H_4SiW_{12}O_{40}\cdot n\,H_2O$[27] (0.75 g) and CH_3COOK (0.50 g) were dissolved in methanol (200 mL; solution B). Solution B was added to solution A with vigorous stirring, and the resulting solution was kept at room temperature for 24 h. Brown

crystals of $K_2[Cr_3O(OOCH)_6(4\text{-ethylpyridine})_3]_2[\alpha\text{-}SiW_{12}O_{40}]\cdot 4\,CH_3OH$ ($\mathbf{1}\cdot 4\,CH_3OH$) were isolated in about 60% yield. FTIR: 1641 (br, $\nu_{asym}(CO_2)$), 1378 (m, $\nu_{sym}(CO_2)$), 972 (m, $\nu_{asym}(W{=}O)$), 924 (s, $\nu_{asym}(Si{-}O)$), 887 (w, $\nu_{asym}(W\text{-}O_c\text{-}W)$), 803 (br, $\nu_{asym}(W\text{-}O_e\text{-}W)$), 636 cm^{-1} (m, $\nu_{asym}(Cr_3O)$). Elemental analysis calcd(%) for $\mathbf{1}\cdot 4\,CH_3OH$: C 15.12, H 1.79, N 1.82, Cr 6.77, K 1.70, Si 0.61, W 47.88; found: C 14.68, H 1.81, N 1.65, Cr 6.58, K 1.68, Si 0.58, W 46.00. TG-DTA spectra of $\mathbf{1}\cdot 4\,CH_3OH$ under dry He flow showed complete removal of methanol molecules at 373 K (Supporting Information, Figure S1). Therefore, the guest-free phase **1** was obtained by the treatment of $\mathbf{1}\cdot 4\,CH_3OH$ at 373 K in vacuo.

X-ray diffraction data of $\mathbf{1}\cdot 4\,CH_3OH$ were collected at 193(1) K with a CCD 2-D detector by using a Rigaku Saturn diffractometer with graphite-monochromated $Mo_{K\alpha}$ radiation ($\lambda = 0.71069$ Å). Data reduction and empirical absorption correction were performed with the HKL2000 package. The structure was solved by direct methods, expanded using Fourier techniques, and refined by full-matrix least-squares against F^2 with the CrystalStructure software package (Rigaku/MSC). Three crystallographically independent potassium ions (K1, K2, and K3) were located with occupancies of 0.6, 0.5, and 0.4, respectively. Four oxygen atoms of the SiO_4 unit in the silicododecatungstate were disordered within eight positions with occupancy of 0.5. Hydrogen atoms were not included in the calculation. Potassium, silicon, chromium, and tungsten atoms were refined anisotropically, while the other atoms were refined isotropically. The potential solvent area of $\mathbf{1}\cdot 4\,CH_3OH$ was calculated with PLATON by including the geometrically located hydrogen atoms.[14] Crystal data of $\mathbf{1}\cdot 4\,CH_3OH$: monoclinic $C2/c$, $a = 32.2376(2)$, $b = 25.4443(2)$, $c = 13.9464(2)$ Å, $\beta = 110.0387(5)°$, $V = 10747.17(19)$ Å^3, $Z = 4$, $D_{calcd} = 2.796\ g\,cm^{-3}$, crystal size $0.20 \times 0.20 \times 0.15\ mm^3$, $T = 193(1)$ K, $\mu(Mo_{K\alpha}) = 13.569\ cm^{-1}$, 14028 reflections collected, 385 parameters, $R_1[I > 2\sigma(I)] = 0.0748$, $wR_2 = 0.2217$, GOF = 1.239. CCDC 852918 contains the supplementary crystallographic data for this paper. These data can be obtained free of charge from The Cambridge Crystallographic Data Centre via www.ccdc.cam.ac.uk/data_request/cif.

Powder X-ray diffraction (XRD) patterns were measured with a SmartLab (Rigaku Corporation) by using $Cu_{K\alpha}$ radiation ($\lambda = 1.54056$ Å, 45 kV–200 mA) in a glass capillary at 0.02° point. The XRD pattern of **1** (298 K) was measured under vacuum, and those of $\mathbf{1}\cdot 0.6\,CO_2$ (299 K, 50 kPa), $\mathbf{1}\cdot 1.5\,CO_2$ (298 K, 110 kPa), $\mathbf{1}\cdot 3\,CO_2$ (233 K, 80 kPa), and $\mathbf{1}\cdot 0.4\,C_2H_2$ (298 K, 90 kPa) were measured under CO_2 and C_2H_2 atmospheres as appropriate. Lattice parameters were calculated using Materials Studio Softwares (Accelrys Inc.) by unit-cell indexing and space-group determination with X-cell followed by peak profile fitting using Pawley refinement.[15,16] The crystal structure of **1** was solved by Rietveld refinement[17] by utilizing the single-crystal structure of $\mathbf{1}\cdot 4\,CH_3OH$ as an initial structure.

Received: November 9, 2011
Published online: January 3, 2012

Keywords: carbon dioxide · ionic crystals · microporous materials · organic–inorganic hybrid composites · polyoxometalates

[1] a) D. M. D'Alessandro, B. Smit, J. R. Long, *Angew. Chem.* **2010**, *122*, 6194; *Angew. Chem. Int. Ed.* **2010**, *49*, 6058; b) D. Aaron, C. Tsouris, *Sep. Sci. Technol.* **2005**, *40*, 321.

[2] a) P. Pässler, W. Hefner, K. Buckl, H. Meinass, A. Meiswinkel, H.-J. Wernicke, G. Ebersberg, R. Müller, J. Bässler, H. Behringer, D. Mayer, *Acetylene. Ullmann's Encyclopedia of Industrial Chemistry*, Wiley-VCH, Weinheim, **2008**; b) P. J. Stang, F. Diederich, *Modern Acetylene Chemistry*, Wiley-VCH, New York, **1995**; c) J. C. W. Chien, *Polyacetylene: Chemistry, Physics and Material Science* Academic Press, New York, **1984**; d) Z. Zhang, S. Xiang, B. Chen, *CrystEngComm* **2011**, *13*, 5983.

[3] a) D. Britt, H. Furukawa, B. Wang, T. G. Glover, O. M. Yaghi, *Proc. Natl. Acad. Sci. USA* **2009**, *106*, 20637; b) D. Saha, Z. Bao, F. Jia, S. Deng, *Environ. Sci. Technol.* **2010**, *44*, 1820; c) M. A. Carreon, S. Li, J. L. Falconer, R. D. Noble, *J. Am. Chem. Soc.* **2008**, *130*, 5412.

[4] a) D. W. Breck, W. G. Eversole, R. M. Milton, T. B. Reed, T. L. Thomas, *J. Am. Chem. Soc.* **1956**, *78*, 5963; b) C. R. Reid, K. M. Thomas, *Langmuir* **1999**, *15*, 3206; c) B. L. Newalkar, N. V. Choudary, U. T. Turaga, R. P. Vijayalakshmi, P. Kumar, S. Komarneni, T. S. G. Bhat, *Microporous Mesoporous Mater.* **2003**, *65*, 267.

[5] a) N. L. Rosi, J. Eckert, M. Eddaoudi, D. T. Vodak, J. Kim, M. O'Keeffe, O. M. Yaghi, *Science* **2003**, *300*, 1127; b) G. Férey, *Chem. Soc. Rev.* **2008**, *37*, 191; c) P. D. C. Dietzel, B. Panella, M. Hirscher, R. Bloma, H. Fjellvåg, *Chem. Commun.* **2006**, 959; d) J.-R. Li, R. J. Kuppler, H.-C. Zhou, *Chem. Soc. Rev.* **2009**, *38*, 1477; e) K. L. Mulfort, J. T. Hupp, *J. Am. Chem. Soc.* **2007**, *129*, 9604; f) X. Lin, I. Telepeni, A. J. Blake, A. Dailly, C. M. Brown, J. M. Simmons, M. Zoppi, G. S. Walker, K. M. Thomas, T. J. Mays, P. Hubberstey, N. R. Champness, M. Schröder, *J. Am. Chem. Soc.* **2009**, *131*, 2159; g) J. W. Yoon, S. H. Jhung, Y. K. Hwang, S. M. Humphrey, P. T. Wood, J.-S. Chang, *Adv. Mater.* **2007**, *19*, 1830.

[6] a) S. Shimomura, M. Higuchi, R. Matsuda, K. Yoneda, Y. Hijikata, Y. Kubota, Y. Mita, J. Kim, M. Takata, S. Kitagawa, *Nat. Chem.* **2010**, *2*, 633; b) B. Xiao, P. J. Byrne, P. S. Wheatley, D. S. Wragg, X. Zhao, A. J. Fletcher, K. M. Thomas, L. Peters, J. S. O. Evans, J. E. Warren, W. Zhou, R. E. Morris, *Nat. Chem.* **2009**, *1*, 289; c) P. L. Llewellyn, S. Bourrelly, C. Serre, Y. Filinchuk, G. Férey, *Angew. Chem.* **2006**, *118*, 7915; *Angew. Chem. Int. Ed.* **2006**, *45*, 7751; d) X. Zhao, B. Xiao, A. J. Fletcher, K. M. Thomas, D. Bradshaw, M. J. Rosseinsky, *Science* **2004**, *306*, 1012.

[7] R. Matsuda, R. Kitaura, S. Kitagawa, Y. Kubota, R. V. Belosludov, T. C. Kobayashi, H. Sakamoto, T. Chiba, M. Takata, Y. Kawazoe, Y. Mita, *Nature* **2005**, *436*, 238.

[8] S. Xiang, W. Zhou, J. M. Gallegos, Y. Liu, B. Chen, *J. Am. Chem. Soc.* **2009**, *131*, 12415.

[9] a) D. G. Samsonenko, H. Kim, Y. Sun, G.-H. Kim, H.-S. Lee, K. Kim, *Chem. Asian J.* **2007**, *2*, 484; b) J.-P. Zhang, X.-M. Chen, *J. Am. Chem. Soc.* **2009**, *131*, 5516.

[10] a) S. Noro, D. Tanaka, H. Sakamoto, S. Shimomura, S. Kitagawa, S. Takeda, K. Uemura, H. Kita, T. Akutagawa, T. Nakamura, *Chem. Mater.* **2009**, *21*, 3346; b) N. Yanai, K. Kitayama, Y. Hijikata, H. Sato, R. Matsuda, Y. Kubota, M. Takata, M. Mizuno, T. Uemura, S. Kitagawa, *Nat. Mater.* **2011**, *10*, 787.

[11] a) Y. Ishii, Y. Takenaka, K. Konishi, *Angew. Chem.* **2004**, *116*, 2756; *Angew. Chem. Int. Ed.* **2004**, *43*, 2702; b) H. Tagami, S. Uchida, N. Mizuno, *Angew. Chem.* **2009**, *121*, 6276; *Angew. Chem. Int. Ed.* **2009**, *48*, 6160; c) S. Uchida, R. Kawamoto, H. Tagami, Y. Nakagawa, N. Mizuno, *J. Am. Chem. Soc.* **2008**, *130*, 12370; d) S. Takamizawa, T. Akatsuka, T. Ueda, *Angew. Chem.* **2008**, *120*, 1713; *Angew. Chem. Int. Ed.* **2008**, *47*, 1689; e) J.-B. Lin, W. Xue, J.-P. Zhang, X.-M. Chen, *Chem. Commun.* **2011**, *47*, 926.

[12] The electrostatic potential (ESP) charges are among the most reliable and commonly used in molecular mechanics and molecular dynamics simulations, and can reproduce the intermolecular interaction properties well: a) U. C. Singh, P. A. Kollman, *J. Comput. Chem.* **1984**, *5*, 129; b) B. H. Besler, K. M. Merz, Jr., P. A. Kollman, *J. Comput. Chem.* **1990**, *11*, 431.

[13] For reviews on POMs, see a) M. T. Pope, A. Müller, *Angew. Chem.* **1991**, *103*, 56; *Angew. Chem. Int. Ed. Engl.* **1991**, *30*, 34; b) C. L. Hill, C. M. Prosser-McCartha, *Coord. Chem. Rev.* **1995**, *143*, 407; c) T. Okuhara, N. Mizuno, M. Misono, *Adv. Catal.* **1996**,

41, 113; d) C. L. Hill, *Chem. Rev.* **1998**, *98*, 1; e) D. Long, E. Burkholder, L. Cronin, *Chem. Soc. Rev.* **2007**, *36*, 105; f) *Polyoxometalate Chemistry for Nano-Composite Design* (Eds.: T. Yamase, M. T. Pope), Kluwer, Dordrecht, **2002**; g) I. V. Kozhevnikov, *Catalysis by Polyoxometalates*, Wiley, Chichester, UK, **2002**; h) C. L. Hill in *Comprehensive Coordination Chemistry II* (Eds.: J. A. McCleverty, T. J. Meyer), Elsevier, Amsterdam, **2004**, p. 679; i) R. Neumann in *Modern Oxidation Methods* (Ed.: J. E. Bäckvall), Wiley-VCH, Weinheim, **2004**, p. 223; j) N. Mizuno, K. Kamata, K. Yamaguchi, *Surface and Nanomolecular Catalysis*, Taylor and Francis Group, New York, **2006**, p. 463.

[14] A. L. Spek, *PLATON, A Multipurpose Crystallographic Tool*, Utrecht University, The Netherlands, **1980**.

[15] M. A. Neumann, *J. Appl. Cryst.* **2003**, *36*, 356.

[16] G. S. Pawley, *J. Appl. Cryst.* **1981**, *14*, 357.

[17] H. M. Rietveld, *J. Appl. Cryst.* **1969**, *2*, 65.

[18] A. Kondo, H. Noguchi, L. Carlucci, D. M. Proserpio, G. Ciani, H. Kajiro, T. Ohba, H. Kanoh, K. Kaneko, *J. Am. Chem. Soc.* **2007**, *129*, 12362.

[19] F. Salles, G. Maurin, C. Serre, P. L. Llewellyn, C. Knöfel, H. J. Choi, Y. Filinchuk, L. Oliviero, A. Vimont, J. R. Long, G. Férey, *J. Am. Chem. Soc.* **2010**, *132*, 13782.

[20] Sorption enthalpy plots of CO_2 and C_2H_2 were calculated with the isotherms at 263–303 K and 273–303 K, respectively, according to the Clausius–Clapeyron equation.[21] The entire plot of CO_2 was obtained by averaging multiple raw plots calculated from two isotherms.

[21] D. W. Breck, *Zeolite Molecular Sieves*, Wiley, New York, **1974**.

[22] a) S. Cavenati, C. A. Grande, A. E. Rodrigues, *J. Chem. Eng. Data* **2004**, *49*, 1095; b) M. E. Rivera-Ramos, G. J. Ruiz-Mercado, A. J. Hernández-Maldonado, *Ind. Eng. Chem. Res.* **2008**, *47*, 5602.

[23] The XRD pattern of **1** did not change with the temperature, showing that changes in the XRD patterns resulted from the increase in the amounts of guest sorption.

[24] At the sorbed amount of 1.5 mol mol^{-1} (298 K, 110 kPa), a new diffraction peak at $2\theta = 7.5°$ appeared, which could not be indexed to a unique crystal lattice (Supporting Information, Figure S6). The intensity of this peak decreased with an increase in the amount of sorption, and the structure converged to a single phase at 3 mol mol^{-1} of the saturated amount of CO_2 sorption (see Figure 2d, 3a). The appearance of the new peak can be ascribed to formation of a transient phase in dynamic phase transition, as has been reported in: a) Y. Kubota, M. Takata, R. Matsuda, R. Kitaura, S. Kitagawa, T. C. Kobayashi, *Angew. Chem.* **2006**, *118*, 5054; *Angew. Chem. Int. Ed.* **2006**, *45*, 4932; b) S. Henke, D. C. F. Wieland, M. Meilikhov, M. Paulus, C. Sternemann, K. Yusenko, R. A. Fischer, *CrystEngComm* **2011**, *13*, 6399.

[25] Since the saturated amount of CO_2 sorption was 3 mol mol^{-1} (see Figure 3a), the CO_2 sorption site above 2 mol mol^{-1} was investigated by in situ IR spectroscopy (Supporting Information, Figure S10). At the sorbed amount of 2.3 mol mol^{-1} (278 K, 93.3 kPa), the intensity of the ν_{as}(W=O) band at 970 cm^{-1} decreased, slightly broadened, and shifted to lower wavenumber. Therefore, CO_2 molecules above the sorbed amount of 2 mol mol^{-1} would interact with the oxygen atoms of silicododecatungstates exposed to the channel walls (blue dashed circle in Figure 1a).

[26] M. K. Johnson, D. B. Powell, R. D. Cannon, *Spectrochim. Acta Part A* **1981**, *37*, 995.

[27] A. Tézé, G. Hervé, *Inorg. Synth.* **1990**, *27*, 93.

